

ON THE TIDAL ORIGIN OF HOT JUPITER STELLAR OBLIQUITY TRENDS

REBEKAH I. DAWSON¹

Department of Astronomy, University of California, Berkeley, Hearst Field Annex, Berkeley CA 94720-3411

Submitted to ApJL on April 10, 2014. Accepted on June 6, 2014.

ABSTRACT

It is debated whether the two hot Jupiter populations — those on orbits misaligned from their host star’s spin axis and those well-aligned — result from two migration channels or from two tidal realignment regimes. Here I demonstrate that equilibrium tides raised by a planet on its star can account for three observed spin-orbit alignment trends: the aligned orbits of hot Jupiters orbiting cool stars, the planetary mass cut-off for retrograde planets, and the stratification by planet mass of cool host stars’ rotation frequencies. The first trend can be caused by strong versus weak magnetic braking (the Kraft break), rather than realignment of the star’s convective envelope versus the entire star. The second trend can result from a small effective stellar moment of inertia participating in the tidal realignment in hot stars, enabling massive retrograde planets to partially realign to become prograde. The third trend is attributable to higher mass planets more effectively counteracting braking to spin up their stars. Both hot and cool star require a small effective stellar moment of inertia participating in the tidal realignment, e.g., an outer layer weakly coupled to the interior. I demonstrate via Monte Carlo that this model can match the observed trends and distributions of sky-projected misalignments and stellar rotation frequencies. I discuss implications for inferring hot Jupiter migration mechanisms from obliquities, emphasizing that even hot stars do not constitute a pristine sample.

Subject headings: planet-star interactions

1. INTRODUCTION

The distribution of host star obliquities ψ — the angle between a planet’s orbital angular momentum and its host star’s spin angular momentum — constrains hot Jupiters’ origin. Hot Jupiters are thought to form at several AU (Rafikov 2006), reaching orbital periods P of several days via: a) high eccentricity migration, in which a Jupiter’s initially highly eccentric orbit shrinks and circularizes because of tidal dissipation in the planet, or b) disk migration (e.g., Goldreich & Tremaine 1980). Mechanisms for the former produce a broad ψ distribution (e.g., Fabrycky & Tremaine 2007; Naoz et al. 2011; Chatterjee et al. 2008), whereas the latter preserves $\psi = 0$ (e.g., Bitsch et al. 2013), unless the disk or star becomes misaligned (Tremaine 1991; Batygin 2012; Rogers et al. 2012; Lai 2014). Rossiter-McLaughlin measurements of λ (Rossiter 1924; McLaughlin 1924) (ψ sky-projected) could distinguish the mechanism of hot Jupiter migration (Morton & Johnson 2011; Naoz et al. 2012) but ψ is sculpted also by tidal dissipation in the star, through which the planet transfers angular momentum from its orbit to the star’s spin.

From early obliquity measurements, Fabrycky & Winn (2009) (FW09 hereafter) inferred two hot Jupiter populations: well-aligned and isotropic. Subsequent discoveries linked them to host stars’ properties: hosts of misaligned Jupiters have effective temperature $T_{\text{eff}} > 6250\text{K}$ (Winn et al. 2010, W10 hereafter) and $M > 1.2M_{\odot}$ (Schlaufman 2010). Among hosts with $M > 1.2M_{\odot}$, those older than 2-2.5 Gyr are aligned, the age at which such stars develop a significant convective envelope (Triaud et al. 2013). W10 proposed that tidal dissipation is more efficient in cool stars with thick convective

envelopes, allowing realignment. Albrecht et al. (2012) (A12 hereafter) confirmed the temperature break with a larger sample, constructed a tidal dissipation parameter, and demonstrated that misalignment is correlated with that parameter. To allow the realignment to occur on timescale shorter than the planet’s orbital decay, W10 suggested that the convective envelopes of cool stars may be sufficiently decoupled from the radiative interior to be realigned separately. Even without stronger dissipation, this decoupling would result in a much shorter timescale for the realignment of cool stars than hot stars.

In the W10 framework, only cool stars experience realignment of their convective envelopes. However, hot Jupiters may also influence the outer layers of hot stars. Hot stars have convective envelopes, which are thinner and therefore arguably easier to realign. For example, a hot Jupiter has synchronized hot star ($T_{\text{eff}} = 6387\text{K}$) τ Bootis, accomplishable if the star has a thin convective envelope weakly coupled to the interior (Catala et al. 2007). A second obliquity trend, the mass cut-off for retrograde planets (e.g., Hébrard et al. 2011), may further be evidence that hot stars are not immune to their hot Jupiters’ tidal influence. Furthermore, attempts to reproduce the observed trends have resulted in major inconsistencies, such as a missing population of $\psi = 180^\circ$ planets or too many oblique cool stars (e.g., Lai 2012; Rogers & Lin 2013; Xue et al. 2014), although individual systems are modeled successfully (Valsecchi & Rasio 2014; Hansen 2012) and λ correlates with the theoretical tidal realignment timescale (A12, Hansen 2012). Here I reconsider the cause of the observed trends. In §2, I summarize the observations, quantifying the temperature cut-off and linking it to the onset of magnetic braking, which I identify from the McQuillan et al. (2014) sample of *Kepler* rotation periods. In §3, I show that

¹ rdawson@berkeley.edu; Miller Fellow

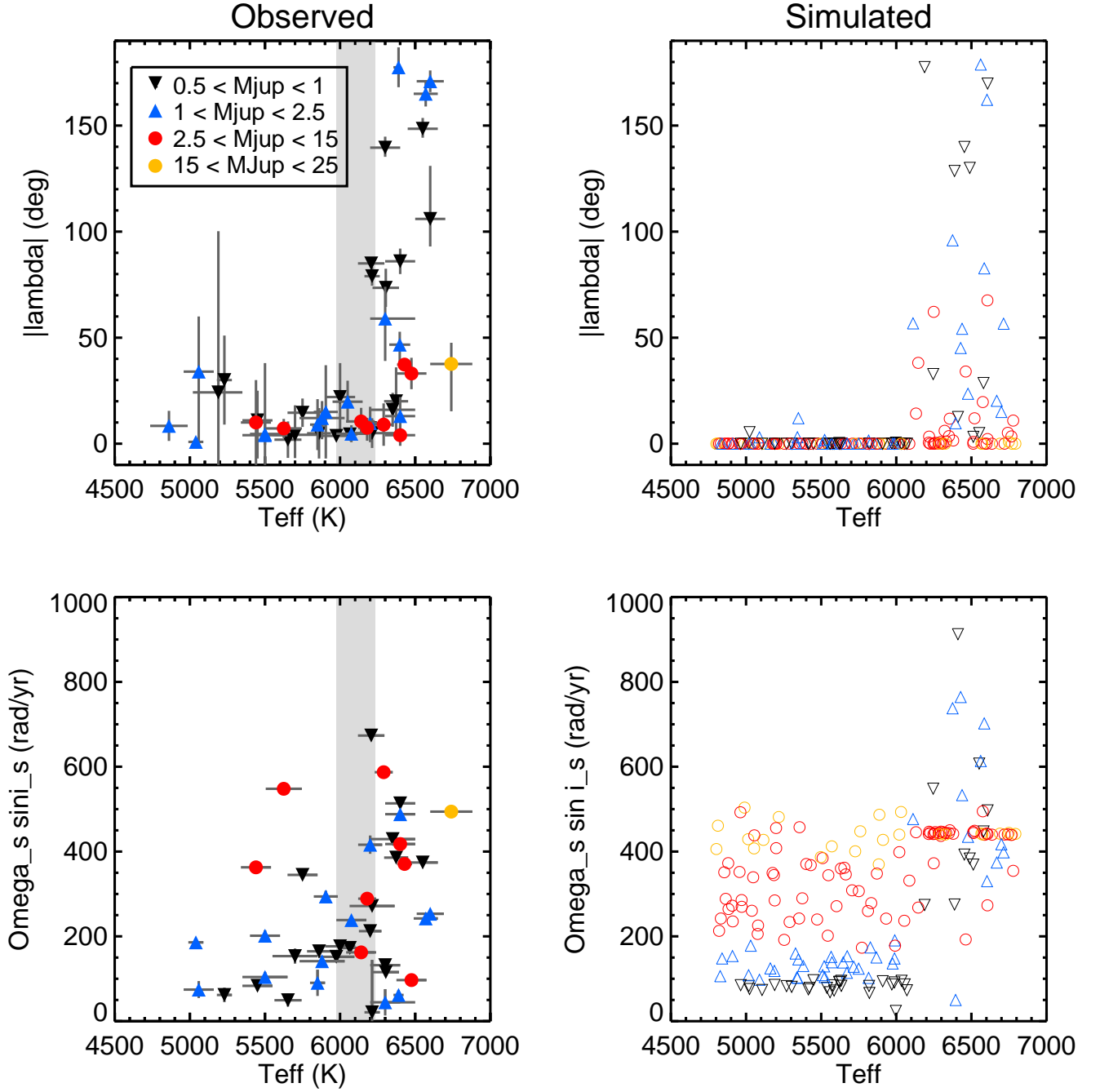


FIG. 1.— Left: Observed sky-projected spin-orbit alignment (λ) and rotation frequencies $\Omega_s = v \sin i_s / R_*$ (Wright et al. 2011, A12). Right: Simulated population (§4).

Eggleton & Kiseleva-Eggleton (2001) equilibrium tides combined with magnetic braking lead to different timescales for orbital decay, spin-orbit alignment, and retrograde flips, producing the observed trends. In §4, I demonstrate via Monte Carlo that the tidal evolution defined in §3 matches the observed trends and distributions. In §5, I summarize the main features of the framework presented and discuss implications for discerning hot Jupiter migration mechanisms.

2. OBSERVED SPIN-ORBIT ALIGNMENT TRENDS

I wish to explain: a) the host star effective temperature cut-off T_{cut} for misaligned planets (W10), and b) the mass cut-off $M_{p,\text{retro}}$ for retrograde planets (Hébrard et al. 2011). Fig. 1 (left panels) displays λ for hot Jupiters² and the host stars' projected stellar rotation frequency $\Omega_\star \sin i_\star$ (computed from $v \sin i_\star$, measured from spectral line broadening, and R_\star) versus T_{eff} . (I plot $\Omega_\star \sin i_\star$ instead of $v \sin i_\star$ for comparison with the simulations in §3.) I note that, particularly below T_{cut} , stars hosting more massive planets have larger rotation frequencies (Fig. 1, bottom left). Due to the scarcity of massive hot Jupiters, the two trends relating to planetary mass are less robust than that with stellar temperature. Above T_{cut} , the chance occurrence that of the twelve significant obliquities, the three lowest correspond to the most massive planets is $\frac{12!3!}{15!} = 0.2\%$; below T_{cut} , the chance occurrence that of the nineteen $\Omega_\star \sin i_\star$, the two highest correspond to the most massive planets is $\frac{17!2!}{19!} = 0.6\%$. These formal estimates of significance do not account for the variety of other patterns we might have observed³, which lowers their true significance.

As A12 showed (Fig. 20), because T_{cut} for λ is also a cut-off for $v \sin i$ (or, plotted here, $\Omega_\star \sin i$), it may correspond to the magnetic braking cut-off. This cut-off is equivalent to gyrochronological Kraft Break for stellar rotation period versus color (Kraft 1967). Braking is thought to be strongest for stars with thick convective envelopes (Schatzman 1962). Therefore A12 interpreted the correspondence of T_{cut} for Ω_\star and ψ as evidence that strong dissipation in the convective envelope plays a role in spin-orbit alignment. I will later argue that magnetic braking, rather than the tidal dissipation efficiency or the participation of the convective envelope versus entire star in tidal realignment, is the cause of T_{cut} for ψ .

I estimate the posterior distribution $\text{prob}(T_{\text{cut}})$ using a model with $\psi = 0$ below T_{cut} and isotropic above (following FW09 except assigning membership to the aligned versus isotropic population based on T_{cut}):

² Defined as $M_p > 0.5 M_{\text{Jup}}$ and $P < 7$ days. These criteria exclude three exceptions to the T_{eff} trend: low mass HAT-P-11-b (Winn et al. 2010) and long period WASP-8-b (Queloz et al. 2010) and HD-80606-b (Moutou et al. 2009). WASP-80-b, a $0.5 M_{\text{Jup}}$ planet orbiting a 4150 K star, would also be an exception, but its spin-orbit alignment remains under investigation (Triaud et al. 2013). I exclude measurements that A12 characterizes as poorly-constrained: CoRoT-1, CoRoT-11, CoRoT-19, HAT-P-16, WASP-2, WASP-23, XO-2. I only include stars with $T_{\text{eff}} < 6800$ K, which excludes KOI-13b.

³ In the case of the mass stratification, I noticed the pattern in my simulations (§3) before I examined the collection of observed Ω_\star .

$$\begin{aligned} \text{prob}(T_{\text{cut}}) = & \prod_i^{N_{\text{planets}}} (\text{prob}(\lambda_i = 0) \text{prob}(T_{\text{eff}i} < T_{\text{cut}}) \\ & + \int_0^\pi d\lambda_i d\psi \text{prob}(\lambda_i|\psi) \\ & \text{prob}(\psi) \text{prob}\lambda_i \text{prob}(T_{\text{eff}i} > T_{\text{cut}})) \end{aligned} \quad (1)$$

for which $\text{prob}(\lambda_i|\psi)$ is FW09 Eqn. 19, $\text{prob}(\psi) = \frac{1}{2} \sin \psi$, and $\text{prob}(T_{\text{eff}})$ and $\text{prob}(\lambda_i)$ are normal distributions defined by their reported uncertainties. I plot $\text{prob}(T_{\text{cut}})$, peaking at 6090_{-110}^{+150} K, and rotation rates measured by McQuillan et al. (2014) for $\sim 10,000$ *Kepler* targets (Fig. 2). The turnover in rotation rate is the Kraft Break; stars above this temperature remain rapidly rotating due to weaker magnetic braking. The Kraft Break matches the peak of $\text{prob}(T_{\text{cut}})$.

3. ORIGIN OF THE TRENDS

I hypothesize on the origin of the observed trends from the equations governing the planet's specific orbital angular momentum vector \vec{h} [length²/time] and the host star's spin angular frequency vector $\vec{\Omega}_\star$ [time⁻¹] (Eggleton & Kiseleva-Eggleton 2001, Eqn. 2–3). I assume the planet's orbit is circular, neglect terms that only cause orbital precession, and add a braking term (Verbunt & Zwaan 1981, Eqn. 4; employed by Barker & Ogilvie 2009 and W10). Equations 2–3 here correspond to Barker & Ogilvie (2009), Eqn. A7 and A12 with the eccentricity vector $\vec{e} = 0$.

$$\dot{\vec{h}} = -\frac{1}{\tau} \frac{\vec{h}}{h} + \frac{1}{\tau} \frac{\Omega_\star}{2n} \left(\frac{\vec{\Omega}_\star \cdot \vec{h}}{\Omega_\star h} \cdot \frac{\vec{h}}{h} + \frac{\vec{\Omega}_\star}{\Omega_\star} \right) \quad (2)$$

$$\dot{\vec{\Omega}}_\star = -\frac{M_p}{I_{\star, \text{eff}}} \dot{\vec{h}} - \alpha_{\text{brake}} \Omega_\star^2 \vec{\Omega}_\star \quad (3)$$

for which

$$\begin{aligned} \tau = & \frac{Q}{6k_L} \frac{M_\star}{R_\star^5 (M_\star + M_p)^8 G^7} \frac{M_\star}{M_p} h^{13} \\ = & \tau_0 \left(\frac{h}{h_0} \right)^{13} \frac{0.5 M_{\text{Jup}}}{M_p} \end{aligned} \quad (4)$$

is an orbital decay timescale, k_L is the Love number, Q is the tidal quality factor, M_p is the planet mass, $I_{\star, \text{eff}}$ is the effective stellar moment of inertia participating in the tidal realignment, α_{brake} is a braking constant, and $h_0 = \sqrt{a_0 G (M_\star + M_p)}$ is the initial specific angular momentum. In the simplified model here, τ_0 is a constant. The timescale τ is related to Eggleton & Kiseleva-Eggleton (2001) Eqn. 7 by replacing the viscous timescale with Q (Eqn. A10), altering the semi-major axis scaling from a^8 to $a^{13/2}$.

The spin-orbit alignment angle, $\cos \psi = \frac{(\vec{h} \times \vec{\Omega}_\star)}{h \Omega_\star}$, evolves according to:

$$\dot{\psi} = -\frac{1}{\tau_{\text{align}}} \sin \psi \left[1 - \frac{\Omega_\star}{2n} \left(\cos \psi - \frac{\tau_{\text{align}}}{\tau} \right) \right] \quad (5)$$

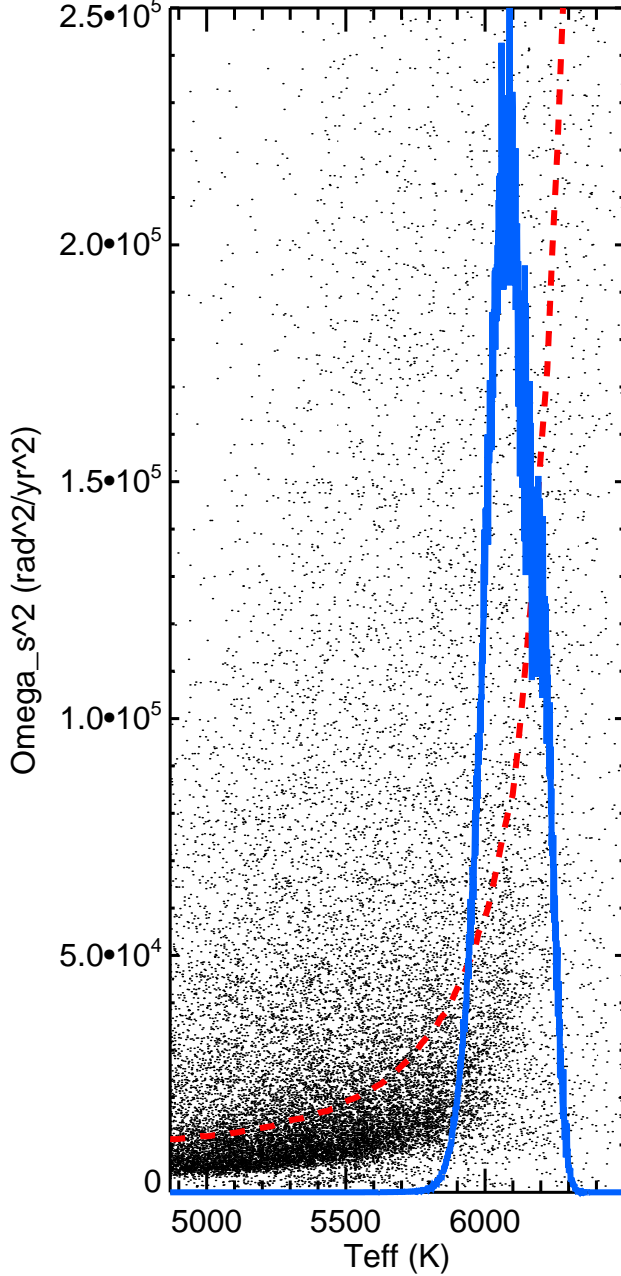


FIG. 2.— Black dots: Squared stellar rotation rates Ω_\star^2 ($0.8 < M_\star < 1.3 M_\odot$) measured by McQuillan et al. (2014). Red dashed line: Running median Ω_\star^2 , binning with $0.06 \text{ dex } \log_{10} T_{\text{eff}}$. Blue solid line: $\text{prob}(T_{\text{cut}})$ from observed λ (Eqn. 1).

with characteristic alignment timescale

$$\tau_{\text{align}} = \frac{\Omega_\star I_{\star, \text{eff}}}{M_p h} \tau, \quad (6)$$

A sharp cut-off in alignment can be produced when ψ accelerates. Neglecting the $\frac{\Omega_\star}{2n}$ term, when h changes slowly compared to ψ ($\tau \gg \tau_{\text{align}}$), ψ accelerates (very approximately) like:

$$\frac{\ddot{\psi}}{\dot{\psi}} \sim \frac{1}{\tau_{\text{brake}}} - \frac{\cos \psi}{\tau_{\text{align}}} \quad (7)$$

for which

$$\tau_{\text{brake}} = \frac{1}{\alpha \Omega_\star^2}, \quad (8)$$

the first term dominates for cool stars, and — for hot stars — the second term leads to quick flips for retrograde planets ($\cos \psi < 0$) and gradual deceleration for prograde planets ($\cos \psi > 0$). Thus τ_{brake} and τ_{align} , when compared to the orbital decay timescale $\tau_{\text{decay}} \sim \tau$ and the star's age ($\tau_{\star, \text{age}}$; more precisely, the time since the hot Jupiter arrived at its close-in location), define tidal evolution regimes leading to the observed trends:

1. Misaligned regime ($\tau_{\text{decay}}, \tau_{\text{brake}}, \tau_{\text{align}} > \tau_{\star, \text{age}}$): \vec{h} and $\vec{\Omega}_\star$ change very little, the **regime for hot Jupiters with $M_p < M_{p, \text{retro}}$ orbiting hot stars** (Fig. 1, black and blue triangles, $T_{\text{eff}} > T_{\text{cut}}$)
2. Flipped regime ($\tau_{\text{decay}}, \tau_{\text{brake}} > \tau_{\star, \text{age}} > \tau_{\text{align}}$): For planets massive enough to cause a short τ_{align} , ψ drops rapidly when the planet's orbit is retrograde ($\cos \psi < 0$, $\frac{\ddot{\psi}}{\dot{\psi}} > 0$), but falls off slowly when prograde ($\cos \psi > 0$, $\frac{\ddot{\psi}}{\dot{\psi}} < 0$), allowing sufficiently massive planets to flip from a retrograde to prograde orbit, the **regime for hot Jupiters with $M_p > M_{p, \text{retro}}$ orbiting hot stars** (Fig. 1, red dots, $T_{\text{eff}} > T_{\text{cut}}$)
3. Realigned regime ($\tau_{\text{decay}} > \tau_{\star, \text{age}} > \tau_{\text{align}_0} > \tau_{\text{brake}}$): braking dominates the ψ acceleration (Equation 7), triggering a fast τ_{align} (due to a small Ω_\star), the **regime for hot Jupiters orbiting cool stars** (Fig. 1, $T_{\text{eff}} < T_{\text{cut}}$)
4. Spin-down regime ($\tau_{\text{decay}}, \tau_{\text{align}} > \tau_{\star, \text{age}} > \tau_{\text{brake}}$): the star slows down but its spin orientation relative to the planet's orbit remains roughly constant ($\dot{\psi} \sim 0$), the **expected regime for low mass planets orbiting cool stars**. HAT-P-11-b (footnote 2, Winn et al. 2010) falls in this category.
5. Fast decay regime ($\tau_{\star, \text{age}} > \tau_{\text{decay}}$): the planet is consumed or tidally disrupted

The $\tau_{\text{align}}/\tau_{\text{decay}}$ ratio is equivalent to the ratio of stellar spin to planetary orbital angular momentum, e.g., employed by Rogers & Lin (2013).

Therefore I argue that the distinction between the hot versus cool stars is not the convective envelope versus entire star participating in the realignment but the host star's rotation rate due to magnetic braking. Although a smaller $I_{\star, \text{eff}}$ for cool stars than for hot stars could in principle cause T_{cut} , hot stars also need a small $I_{\star, \text{eff}}$ for regime 2. Therefore the distinction must be in Ω_\star (§2), which differs systematically (hot stars spin quickly and cool stars slowly) due to a different magnetic braking strength. Furthermore, hot stars need weak magnetic braking for regime 2, whereas cool stars need strong magnetic braking for the planet to tidally realign the star's outer layer of without synchronization (Fig. 1). Therefore I consider strong versus weak magnetic braking to be the cause of the observed trends, in concert with a small $I_{\star, \text{eff}}$ for all stars, corresponding to an outer layer that participates in the tidal realignment while weakly

coupled to the interior. Although in principle a small $I_{\star, \text{eff}}$ is unnecessary if Ω_{\star} is initially extremely small, Ω_{\star} needs to match the observed $\Omega_{\star} \sin i_s$ measurements (Fig. 1, bottom left panel).

I plot several illustrative cases, using the parameters below (Fig. 3). The black dashed lines show a low-mass planet realigning a cool star. The red dashed lines represent a high-mass planet realigning a cool star. The more massive planet spins up the star, resulting in a shorter stellar rotation period. The solid black lines depict a massive planet that orbits a hot star flipping from retrograde to prograde (regime 2), whereas the solid red lines represent a less massive planet inducing little realignment over the host star's lifetime (regime 1). In all cases, the planets experience little orbital decay (top panel).

Using the timescales above, I estimate physical constants that produce the observed regimes. For cool stars to realign and slow to the observed $(\Omega_{\star})_{\text{final}} \sim 225$ rad/yr, strong braking and low $I_{\star, \text{eff}}$ are required:

$$\alpha_{\text{cool}} \sim 3 \times 10^{-13} \text{ yr} \left(\frac{225 \text{ rad/yr}}{(\Omega_{\star})_{\text{final}}} \right)^2 \frac{0.07 \text{ Gyr}}{t_{\text{align}}} \quad (9)$$

$$I_{\star, \text{eff}} \sim 0.0004 M_{\odot} R_{\odot}^2$$

$$\frac{t_{\text{align}}/t_{\text{decay}}}{0.003} \frac{M_p}{0.5 M_{\text{Jup}}} \frac{h_0}{1.33 \text{ AU}^2/\text{yr}} \frac{225 \text{ rad/yr}}{(\Omega_{\star})_{\text{final}}},$$

much smaller than the sun's $I \sim (0.06 M_{\odot} R_{\odot}^2)$.

Next I estimate $I_{\star, \text{eff}}$ for hot stars. For planets with $M_p > M_{p, \text{retro}}$ to flip to prograde, I require:

$$I_{\star, \text{eff}} \sim 0.0019 M_{\odot} R_{\odot}^2$$

$$\frac{\tau_{\text{align}}/t_{\text{decay}}}{0.007} \frac{M_{p, \text{retro}}}{2.5 M_{\text{Jup}}} \frac{h_0}{1.33 \text{ AU}^2/\text{yr}} \frac{600 \text{ rad/yr}}{(\Omega_{\star})_{\text{final}}} \quad (10)$$

Although this corresponds to a slightly larger $I_{\star, \text{eff}}$ than for cool stars, it is still much smaller than the moment of inertia of the entire star (e.g., a $1.2 M_{\odot}$, $1.2 R_{\odot}$ $n = 3$ polytrope has $I = 0.14 M_{\odot} R_{\odot}^2$). In §5, I discuss whether such a small $I_{\star, \text{eff}}$ for either hot or cool stars is plausible.

4. REPRODUCING THE OBSERVED TRENDS

I show via Monte Carlo that the framework from §3 can reproduce the observed trends. I use the constants derived above (Eqn. 9–10) and adopt $\tau_0 = 1000$ Gyr (τ scales with planet mass according to Eqn. 4; τ_0 corresponds to $Q \sim 5 \times 10^6$ for a sun-like star), $(\Omega_{\star})_{0, \text{hot}} = 1000$ rad/yr, $(\Omega_{\star})_{0, \text{cool}} = 400$ rad/yr, $\alpha_{\text{hot}} = 3 \times 10^{-16}$ yr, and $h_0 = 1.33 \text{ AU}^2/\text{yr}$ (corresponding to $P \sim 3$ days, where the hot Jupiter pile-up is observed, e.g., Gaudi et al. 2005). The values are tuned to match the observations (Fig. 1).

To produce a predicted population, for 200 planets I:

1. Select a uniform random $4800 < T_{\text{eff}} < 6800$ K, a log-uniform $0.5 M_{\text{Jup}} < M_p < 25 M_{\text{Jup}}$, and ψ from an isotropic distribution.
2. Select a uniform random evolution time $0 < t < 10$

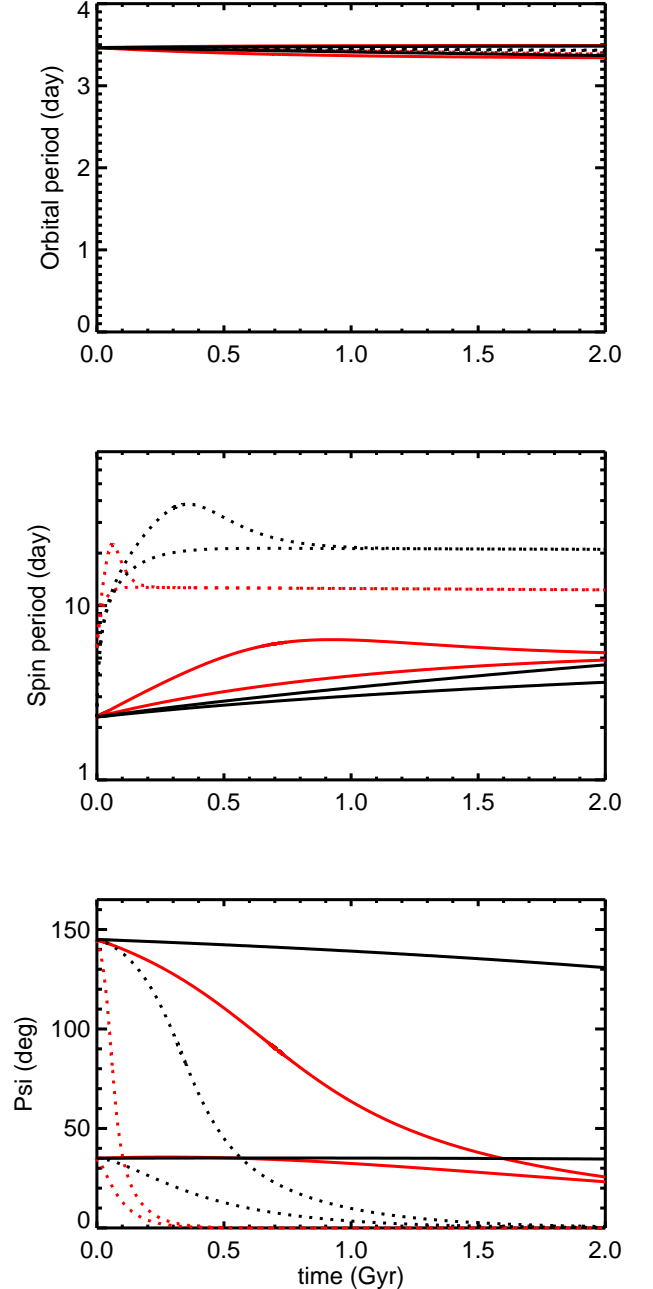


FIG. 3.— Planetary P (top), stellar spin period (middle), and ψ (bottom) for $M_p = 1 M_{\text{Jup}}$ (black) and $M_p = 3 M_{\text{Jup}}$ (red) and hot (solid) or cool (dotted) host stars for an initial misalignment $\psi = 145^\circ$ (corresponding to higher lines with bumps in middle panel) and 35° .

Gyr for cool stars ($T_{\text{cut}} < 6100\text{K}$) or $0 < t < 4$ Gyr for hot stars. Integrate Eqn. 2, 3, and 4 for t .

3. Compute $\psi(t)$ and select a uniform random longitude of ascending node $0 < \Omega < 2\pi$, yielding the sky-projected $\lambda = \tan^{-1}(\tan \psi \sin \Omega)$ (FW09, Eqn. 11).

4. Compute $\sin i_{\star} = \sqrt{1 - (\sin \psi \cos \Omega)^2}$ and $v \sin i_{\star}/R_{\star} = \Omega_{\star} \sin i_{\star}$.

Fig. 1 (right panels) displays simulated planets not

subsumed by their stars (most have P close to the initial value). Qualitatively I match the observed distributions and trends in λ and Ω_* (Fig. 1, left panels): the sharp transition at T_{cut} between aligned and misaligned planets, the mass cut-off for retrograde planets, the larger rotation frequencies for hot stars, and the planet mass stratification of the projected rotation frequencies for cool stars. The mass stratification results from the highest mass planets spinning up their host stars, counteracting magnetic braking.

I repeat the simulation replacing Q with a viscous time constant, such that $\tau \propto h^{16}$: the results do not change noticeably, likely because the planet experiences little orbital decay. I can increase $I_{*, \text{eff}}$ for cool stars to $0.004 M_\odot R_\odot$ by decreasing τ_0 to 100 Gyr for cool stars only, but more planets are tidally disrupted. I cannot more than double $I_{*, \text{eff}}$ for hot stars. The results are not strongly sensitive to the initial P , which mostly affects how much the massive planets spin up their host stars; a longer P also, via the $\frac{\Omega_*}{2n}$ term (Eqn. 5), partially counteracts the realignment. I try to reproduce the observed trends and distributions in several alternative regimes (not shown): large $I_{*, \text{eff}}$ with strong braking or low initial Ω_* , large $I_{*, \text{eff}}$ with initially strong braking that drops after 100 Myr, and weak braking for cool stars but smaller initial Ω_* . I find that although I can reproduce the distribution and trends in λ in these regimes, I cannot simultaneously reproduce the observed $\Omega_* \sin i_s$.

5. CONCLUSION

I advocate that equilibrium tides with magnetic braking and a small effective stellar moment of inertia participating in the tidal realignment ($I_{*, \text{eff}}$) can account for the observed trends and distributions of hot Jupiters' spin-orbit alignments and host star projected rotation frequencies. This framework is based on W10 and A12 but with several modifications to match the observations. The observed temperature cut-off between aligned and misaligned planets is due to stellar magnetic braking, rather than the tidal dissipation efficiency or whether the star's convective envelope is tidally realigned independent of the interior. For cool stars, strong magnetic braking⁴, slows the rotation and lowers the spin angular momentum, allowing the planet to realign the star's outer layer without synchronization. Both hot and cool stars require a $I_{*, \text{eff}}$ 30-100 times lower than the star's total I . For cool stars, magnetic braking shrinks the star's spin vector without changing the direction, so a small $I_{*, \text{eff}}$ allows a smidgen of orbital decay to nudge the star to realignment. For hot stars, a small $I_{*, \text{eff}}$ allows sufficiently massive planets to flip from retrograde to prograde, producing the observed retrograde planetary mass cut-off. Finally, more massive planets partially overcome magnetic braking to spin up the star, leading to the observed planet-mass-stratification of host star rotation frequency for cool stars.

There are several caveats. The observed trends with planet mass are less robust than that with stellar effective temperature due to the rarity of massive hot Jupiters. Therefore Rossiter-McLaughlin measurements of newly

discovered hot Jupiters with $M_p > 2.5 M_{\text{Jup}}$ would be particularly valuable. I assumed that the initial ψ distribution is independent of M_p ; if the retrograde mass-cut were caused by the mechanism leading to misalignment, a small $I_{*, \text{eff}}$ for hot stars would not be necessary. Furthermore, whether such a small $I_{*, \text{eff}}$ — an outer layer participating in the tidal realignment while weakly coupled to the interior — is plausible remains an open question. As proposed by W10, this weakly coupled outer layer could be the convective zone. Following W10, I compute the convective zone I of a 5 Gyr sun-like star and a 2 Gyr 1.2 solar-mass star using the EZ Web stellar evolution models (Paxton 2004): $0.01 M_\odot R_\odot^2$ and $0.002 M_\odot R_\odot^2$ respectively. The latter is consistent with the value estimated here ($0.0019 M_\odot R_\odot^2$). The former is inconsistent with the estimated value $0.0004 M_\odot R_\odot^2$ using nominal parameters and marginally consistent with $0.004 M_\odot R_\odot^2$ if I allow cool stars to have a much shorter orbital decay timescale. The weakly coupled outer layer does not necessarily correspond to the convective zone, just an effective distance for the transferred angular momentum to penetrate. A weakly coupled outer layer would account τ Bootis b synchronizing its hot star. For cool stars, a weakly coupled outer layer seems at odds with the sun's radially uniform rotation profile. One possibility is that the weakly coupled outer layer corresponds to our sun's near-surface shear outer layer at about $0.95 R_\odot$ (e.g., Thompson et al. 1996), which is decoupled from the rest of the convective zone at low latitudes. The depth from the surface probed by λ and $v \sin i_*$ measurements is < 100 km (e.g., Gray 2008). Another possibility is that the timescale for coupling between layers, often treated as a free parameter in tidal evolution models due to uncertainty over which proposed physical process is responsible for coupling (e.g., Allain 1998; Penev et al. 2014), is much longer than the tidal forcing timescale.

I used a simplistic tidal evolution model to illuminate an origin for the observed stellar obliquity trends. Ultimately a detailed, realistic treatment is necessary, incorporating stellar evolution (accounting for age trends, i.e. Triaud 2011), coupling between the star's layers, changes in α_{brake} , dynamic tides, stellar properties affecting tides (e.g., R_* , and tides raised on the planet). The values of physical constants I tuned to match observations — such as the braking coefficient and initial host star spin rate — are not precise constraints due to the model's simplistic treatment, but better models may allow meaningful constraints. For example, a constraint on the initial host star spin rate could pinpoint the star's age when the realignment begins, potentially distinguishing between disk migration (which occurs before the gas disk evaporates) versus high eccentricity migration (which delivers the hot Jupiter over a larger range of timescales).

A key take-away for using the ψ distribution to constrain hot Jupiter migration mechanisms is that cool star obliquities are significantly sculpted by tides, as are hot star obliquities for the more massive hot Jupiters. For example, if one were to take the ψ distribution of hot stars as pristine, one would overestimate the fraction of prograde planets due to the flipping of massive retrograde planets. Better tidal evolution models will allow robustly forward-modeling the migration and tidal sculpting process to match the observed distribution of sky-projected

⁴ Magnetic braking was included in W10's realignment example and highlighted by W10 as enabling realignment without synchronization.

λ.

My gratitude to the referee for an especially helpful report. I thank Joshua Winn, Gwenaél Boué, Eliot Quataert, Daniel Fabrycky, Ryan O’Leary, Eugene Chiang, Simon Albrecht, Amaury Triaud, Marta Bryan,

Howard Isaacson, Ruth Murray-Clay, and Ian Czekala for helpful feedback, comments, and discussions, Ruth Angus for an inspiring presentation on gyrochronology, the Miller Institute for Basic Research in Science, University of California Berkeley for funding, and the Exoplanet Orbit Database (exoplanets.org) .

REFERENCES

- Albrecht, S., Winn, J. N., Johnson, J. A., Howard, A. W., Marcy, G. W., Butler, R. P., Arriagada, P., Crane, J. D., Shectman, S. A., Thompson, I. B., Hirano, T., Bakos, G., & Hartman, J. D. 2012, *ApJ*, 757, 18
- Allain, S. 1998, *A&A*, 333, 629
- Barker, A. J., & Ogilvie, G. I. 2009, *MNRAS*, 395, 2268
- Batygin, K. 2012, *Nature*, 491, 418
- Bitsch, B., Crida, A., Libert, A.-S., & Lega, E. 2013, *A&A*, 555, A124
- Catala, C., Donati, J.-F., Shkolnik, E., Bohlender, D., & Alecian, E. 2007, *MNRAS*, 374, L42
- Chatterjee, S., Ford, E. B., Matsumura, S., & Rasio, F. A. 2008, *ApJ*, 686, 580
- Eggleton, P. P., & Kiseleva-Eggleton, L. 2001, *ApJ*, 562, 1012
- Fabrycky, D., & Tremaine, S. 2007, *ApJ*, 669, 1298
- Fabrycky, D. C., & Winn, J. N. 2009, *ApJ*, 696, 1230
- Gaudi, B. S., Seager, S., & Mallen-Ornelas, G. 2005, *ApJ*, 623, 472
- Goldreich, P., & Tremaine, S. 1980, *ApJ*, 241, 425
- Gray, D. F. 2008, *The Observation and Analysis of Stellar Photospheres*, by David F. Gray, Cambridge, UK: Cambridge University Press, 2008,
- Hansen, B. M. S. 2012, *ApJ*, 757, 6
- Hébrard, G., Ehrenreich, D., Bouchy, F., Delfosse, X., Moutou, C., Arnold, L., Boisse, I., Bonfils, X., Díaz, R. F., Eggenberger, A., Forveille, T., Lagrange, A.-M., Lovis, C., Pepe, F., Perrier, C., Queloz, D., Santerne, A., Santos, N. C., Ségransan, D., Udry, S., & Vidal-Madjar, A. 2011, *A&A*, 527, L11
- Kraft, R. P. 1967, *ApJ*, 150, 551
- Lai, D. 2012, *MNRAS*, 423, 486
- Lai, D. 2014, *MNRAS*, 440, 3532
- McLaughlin, D. B. 1924, *ApJ*, 60, 22
- McQuillan, A., Mazeh, T., & Aigrain, S. 2014, *ApJS*, 211, 24
- Morton, T. D., & Johnson, J. A. 2011, *ApJ*, 729, 138
- Moutou, C., Hébrard, G., Bouchy, F., et al. 2009, *A&A*, 498, L5
- Naoz, S., Farr, W. M., Lithwick, Y., Rasio, F. A., & Teyssandier, J. 2011, *Nature*, 473, 187
- Naoz, S., Farr, W. M., & Rasio, F. A. 2012, *ApJ*, 754, L36
- Paxton, B. 2004, *PASP*, 116, 699
- Penev, K., Zhang, M., & Jackson, B. 2014, *arXiv:1405.1050*
- Queloz, D., Anderson, D. R., Collier Cameron, A., et al. 2010, *A&A*, 517, L1
- Rafikov, R. R. 2006, *ApJ*, 648, 666
- Rogers, T. M., & Lin, D. N. C. 2013, *ApJ*, 769, L10
- Rogers, T. M., Lin, D. N. C., & Lau, H. H. B. 2012, *ApJ*, 758, L6
- Rossiter, R. A. 1924, *ApJ*, 60, 15
- Schatzman, E. 1962, *Annales d’Astrophysique*, 25, 18
- Schlaufman, K. C. 2010, *ApJ*, 719, 602
- Thompson, M. J., Toomre, J., Anderson, E. R., et al. 1996, *Science*, 272, 1300
- Tremaine, S. 1991, *Icarus*, 89, 85
- Triaud, A. H. M. J. 2011, *A&A*, 534, L6
- Triaud, A. H. M. J., Anderson, D. R., Collier Cameron, A., et al. 2013, *A&A*, 551, A80
- Valsecchi, F., & Rasio, F. A. 2014, *ApJ*, 786, 102
- Verbunt, F., & Zwaan, C. 1981, *A&A*, 100, L7
- Winn, J. N., Fabrycky, D., Albrecht, S., & Johnson, J. A. 2010, *ApJ*, 718, L145
- Winn, J. N., Johnson, J. A., Howard, A. W., et al. 2010, *ApJ*, 723, L223
- Wright, J. T., Fakhouri, O., Marcy, G. W., Han, E., Feng, Y., Johnson, J. A., Howard, A. W., Fischer, D. A., Valenti, J. A., Anderson, J., & Piskunov, N. 2011, *PASP*, 123, 412
- Xue, Y., Suto, Y., Taruya, A., Hirano, T., Fujii, Y., & Masuda, K. 2014, *ApJ*, 784, 66